

1 CERN, the LHC, and the CMS Experiment

1.1 CERN and the Large Hadron Collider

The European Council for Nuclear Research (in French *Conseil Européen pour la Recherche Nucléaire*), also known as CERN, is the site of an accelerator complex hosting the Large Hadron Collider (LHC). The LHC consists of a 27-kilometer ring of superconducting magnets with accelerating structures to boost the energy of particles, which collide at a center-of-mass energy of up to 14 TeV. The beams inside the LHC are made to collide at four locations around the accelerator ring, at the locations of four particle detectors: ATLAS, CMS, ALICE, and LHCb.

The number of events generated per second at the LHC collisions is given by $N_{event} = \mathcal{L}\sigma_{event}$, where σ_{event} is the cross-section for the event under study, and \mathcal{L} the machine luminosity. The machine luminosity depends only on the beam parameters, and can be written for a Gaussian beam distribution as:

$$\mathcal{L} = \frac{N_b^2 n_b f_{rev} \gamma_r}{4\pi \epsilon_n \beta^*} F \quad (1)$$

where N_b is the number of particles per bunch, n_b the number of bunches per beam, f_{rev} the revolution frequency, γ_r the relativistic gamma factor, ϵ_n the normalized transverse beam emittance, β^* the beta function at the collision point, and F the geometric luminosity reduction factor due to the crossing angle at the interaction points. Luminosity is measured in units of $\text{cm}^{-2} \text{s}^{-1}$. Thus the exploration of rare events in the LHC collisions requires both high beam energies and high beam intensities.

1.2 The CMS Detector

The Compact Muon Solenoid (CMS) experiment was conceived to study proton-proton and lead-lead collisions at a center-of-mass energy of 14 TeV (5.5 TeV nucleon-nucleon) and at luminosities up to $10^{34} \text{ cm}^{-2} \text{s}^{-1}$ ($10^{27} \text{ cm}^{-2} \text{s}^{-1}$). At the center of the CMS detector, a high-magnetic-field superconducting solenoid surrounds a silicon pixel and strip tracker, a lead-tungstate scintillating-crystals electromagnetic calorimeter (ECAL), and a brass-scintillator sampling hadron calorimeter (HCAL). The iron yoke of the flux-return houses four stations of gas-ionization chamber muon detectors. The collision data is recorded with the use of the Level-1 (L1) trigger, high-level trigger (HLT), and data acquisition systems ensuring high efficiency in selecting physics events of interest. A detailed description of the CMS detector can be found in [CITE].

CMS uses a right-handed coordinate system [CITE]. The origin is centered at the nominal collision point inside the experiment. The x axis points towards the center of the LHC, and the y axis points vertically upwards. The z axis points along the beam direction. The azimuthal angle, ϕ , is measured from the x axis in the x - y plane, and the radial coordinate in this plane is denoted by r . The polar angle, θ , is measured from the z axis. The pseudorapidity, η , is defined as $\eta = -\ln \tan(\theta/2)$. The momentum and energy transverse to the beam direction, denoted by p_T and E_T respectively, are computed from the x and y components. The momentum imbalance in the transverse plane is called the missing transverse momentum, and its magnitude is denoted by E_T^{miss} .

1.3 Sub-detectors of CMS

This section details the sub-detectors of CMS that operate to identify and precisely measure muons, electrons, photons, and jets over a large energy range.

1.3.1 Inner tracking system

The CMS Tracker perform robust tracking and detailed vertex reconstruction in the 4 T magnetic field of the superconducting solenoidal magnet. The active envelope of the CMS Tracker extends to a radius of 115 cm, over a length of approximately 270 cm on each side of the interaction point [CITE]. Charged particles in the region $|\eta| \lesssim 1.6$ benefit from the full momentum measurement precision. In this region, a charged particle with p_T of 1000 GeV has a sagitta of $\sim 195 \mu\text{m}$. The Tracker acceptance extends further to $|\eta| = 2.5$, with a reduced radial lever arm of approximately 50 cm.

The high magnetic field of CMS causes low p_T charged particles to travel in helical trajectories with small radii. The majority of events contain particles with a steeply falling p_T spectrum, resulting in a track density which rapidly decreases at higher radii.

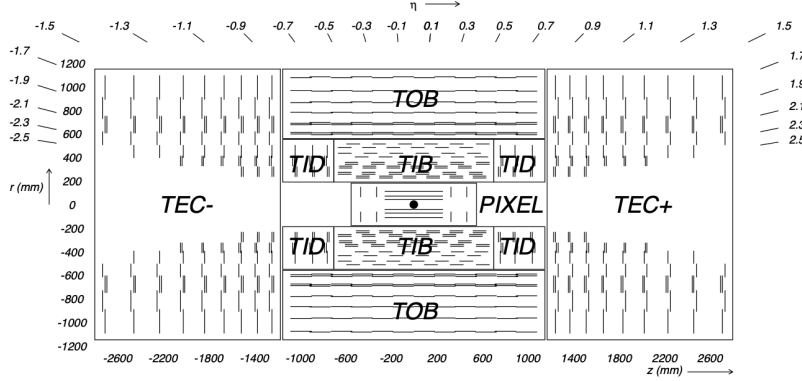


Figure 1: Cross section of the current Phase-1 CMS tracker from [CITE] <https://cds.cern.ch/record/1481838/files/CMS-TDR-011.pdf>, showing the nomenclature of different sections. Each line represents a detector module. Double lines indicate back-to-back modules which deliver stereo hits in the strip tracker.

A schematic view of the current Phase-1 CMS tracker, including the pixel detector, is shown in Fig. 1. The Phase-1 pixel detector consists of three barrel layers (BPIX) at radii of 4.4 cm, 7.3 cm, and 10.2 cm, and two forward/backward disks (FPIX) at longitudinal positions of ± 34.5 cm and ± 46.5 cm, and extending in radius from about 6 cm to 15 cm. These pixelated detectors produce 3D measurements along the paths of charged particles with single hit resolutions between 10-20 μm .

After the pixel and on their way out of the tracker, particles pass through the silicon strip tracker which reaches out to a radius of 130 cm (Fig. 1). The sensor elements in the strip tracker are single-sided p -on- n type silicon micro-strip sensors [CITE 2008 CMS]. The silicon strip detector consists of four inner barrel (TIB) layers assembled in shells, with two inner endcaps (TID), each composed of three small discs. The outer barrel (TOB) consists of six concentric layers. Two endcaps (TEC) close off the tracker on either end.

1.3.2 ECAL

The electromagnetic calorimeter (ECAL) of CMS measures electromagnetic energy deposits with high granularity. One of the driving criteria in the design was the capability of detecting the Standard Model Higgs boson decay to two photons (in fact, the channel in which the 125 GeV Higgs boson was discovered at CMS).

High-energy electrons predominantly lose energy in matter via bremsstrahlung, and high-energy photons by e^+e^- pair production. The characteristic amount of matter traversed for these interactions is called the radiation length X_0 , usually measured in units of g cm^{-2} . It is the mean distance over which a high-energy electron loses all but $1/e$ of its energy via bremsstrahlung [CITE PDG].

ECAL is a hermetic homogenous calorimeter comprised of 61,200 lead tungstate (PbWO_4) crystals mounted in the central barrel, with 7,324 crystals in each of the two endcaps [CITE]. A preshower detector is located in front of the endcap crystals. Avalanche photodiodes (APDs) are used as photodetectors in the barrel and vacuum phototriodes (VPTs) in the endcaps.

The barrel part of the ECAL (EB) covers the pseudorapidity range $|\eta| < 1.479$. The barrel granularity is 360-fold in ϕ and (2×85) -fold in η . The crystal cross-section corresponds to approximately 0.0174×0.0174 in $\eta - \phi$ or $22 \times 22 \text{ mm}^2$ at the front face of the crystal, and $26 \times 26 \text{ mm}^2$ at the rear face. The crystal length is 230 mm, corresponding to $25.8 X_0$.

The ECAL read-out acquires the signals of the photodetectors. At each bunch crossing, digital sums representing the energy deposit in a trigger tower, comprising 5×5 crystals in $\eta \times \phi$, are generated and sent to the Level-1 trigger system (detailed in Section 1.4).

1.3.3 HCAL

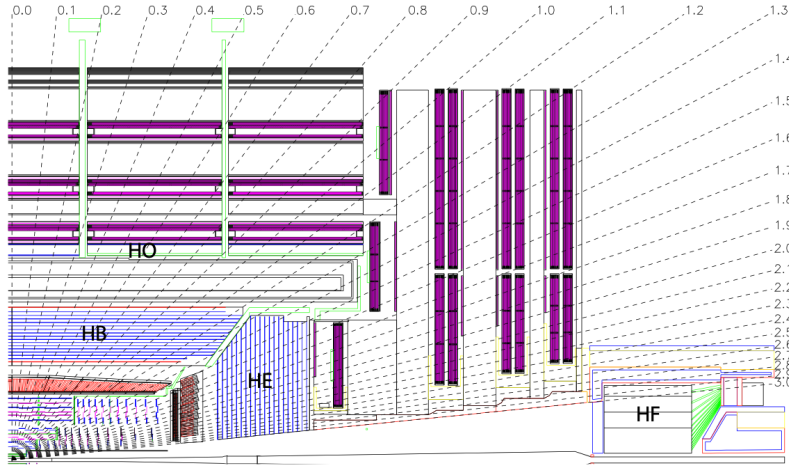


Figure 2: Longitudinal view of the CMS detector showing the hadron calorimeter barrel (HB), endcap (HE), outer (HO), and forward (HF) calorimeters from [CITE 2008 JINST 3 S08004].

The hadronic calorimeter (HCAL) of CMS plays an important role in the measurement of hadron jets and neutrinos or exotic particles resulting in apparent missing transverse energy. A view of the CMS detector showing the components of HCAL is shown in Fig. 2. The HCAL barrel (HB) and endcaps (HE) are located outside of the tracker and the ECAL. The hadron calorimeter barrel is radially restricted between the outer radius of the electromagnetic calorimeter at a radius of 1.77 m, and the inner extent of the magnet coil at radius 2.95 m. An outer hadron calorimeter (HO) is placed outside the solenoid to complement the barrel calorimeter. Beyond $|\eta| = 3$, the forward hadron calorimeter (HF) at 11.2 m from the interaction point extend the pseudorapidity coverage to $|\eta| = 5.2$.

The HB is a sampling calorimeter covering the pseudorapidity range $|\eta| < 1.3$. It consists of 36 identical azimuthal wedges which form two half-barrels (HB+ and HB-). Each wedge is segmented into four azimuthal angle (ϕ) sectors. The plastic scintillator is divided into 16 η sectors, resulting in a segmentation of $(\Delta\eta, \Delta\phi) = (0.087, 0.087)$. The HE covers pseudorapidity $1.3 < |\eta| < 3$, and the design is driven by the need to minimize the cracks between HB and HE, rather than single-particle energy resolution, since the resolution of jets in HE will be limited by pileup, magnetic field effects, and parton fragmentation.

In the central pseudorapidity region, the combined stopping power of EB plus the HB is insufficient to contain hadron showers [CITE]. To ensure adequate sampling depth, the hadron calorimeter is extended with a tail catcher, the HO. The size and position of the tiles are designed to roughly map the layers of the HB to make towers with the same granularity of 0.087×0.087 in η and ϕ . The HO is physically divided in 5 rings in η conforming to the muon ring structure.

The HF is foremost designed to survive in the harsh radiation conditions and high particle flux of the forward region. On average, 760 GeV per proton-proton interaction is deposited into the two forward calorimeters, compared to only 100 GeV for the rest of the detector [CITE]. Furthermore, this energy has a pronounced maximum at the highest rapidities. As a result of these radiation considerations, quartz fibers are used as the active medium. The signal is generated when charged shower particles above the Cherenkov threshold

1.3.4 Muon detectors

1.4 The Level-1 Trigger

1.5 The Phase-2 Upgrade of the CMS detector